Chapter 3

High Electron Mobility Transistors: Performance Analysis, Research Trend and Applications

Muhammad Navid Anjum Aadit,
Sharadindu Gopal Kirtania, Farhana Afrin,
Md. Kawsar Alam and Quazi Deen Mohd Khosru

Additional information is available at the end of the chapter

http://dx.doi.org/10.5772/67796

Abstract

In recent years, high electron mobility transistors (HEMTs) have received extensive attention for their superior electron transport ensuring high speed and high power applications. HEMT devices are competing with and replacing traditional field-effect transistors (FETs) with excellent performance at high frequency, improved power density and satisfactory efficiency. This chapter provides readers with an overview of the performance of some popular and mostly used HEMT devices. The chapter proceeds with different structures of HEMT followed by working principle with graphical illustrations. Device performance is discussed based on existing literature including both analytical and numerical models. Furthermore, some notable latest research works on HEMT devices have been brought into attention followed by prediction of future trends. Comprehensive knowledge of up-to-date results, future directions, and their analysis methodology would be helpful in designing novel HEMT devices.

Keywords: 2DEG, heterojunction, high electron mobility, polarization, power amplifier, quantum confinement

1. Introduction

The requirement of high switching speed such as needed in the field of microwave communications and RF technology urged transistors to evolve with high electron mobility and superior transport characteristics. The invention of HEMT devices is accredited to T. Mimura who was involved in research of high-frequency, high-speed III–V compound semiconductor devices at Fujitsu Laboratories Ltd, Kobe, Japan. Following that, HEMT was first commercially used as a cryogenic low-noise amplifier at Nobeyama Radio Observatory (NRO), Nagano, Japan in 1985 [1].

Working toward the need of high frequency, low noise, and high power density applications, traditional MOSFETs and MESFETs require to be built with very short channel lengths so that majority of the carriers face minimum impurity scattering and performance degradation is reduced. Such applications also imply design and performance limitations requiring high saturation current as well as large transconductance, which may be achieved by heavy doping. To overcome these limitations, HEMT devices incorporate heterojunctions formed between two different bandgap materials where electrons are confined in a quantum well to avoid impurity scattering. The direct bandgap material GaAs have been used in high frequency operation as well as in optoelectronic integrated circuits owing to its higher electron mobility and dielectric constant. AlGaAs are the most suitable candidate for barrier material of GaAs possessing nearly same lattice constant and higher bandgap than that of GaAs. That is why GaAs/AlGaAs heterostructure is considered to be the most popular choice to be incorporated in HEMTs. However, AlGaN/GaN HEMT is another excellent device that has been extensively researched in recent times. It can operate at very high frequencies with satisfactory performance as well as possess high breakdown strength and high electron velocity in saturation [2]. GaN shows very strong piezoelectric polarization which aids accumulation of enormous carriers at AlGaN/GaN interface. In these types of HEMTs, device performance depends on the types of material layer, layer thickness, and doping concentration of AlGaN layer providing flexibility in the design process. For its superiority over HEMT devices with other materials, AlGaN/GaN HEMT has been selected as an example for different topics in this chapter.

The chapter begins with brief explanation of different common structures and basic operating principle of HEMT devices. The main focus is to analyze HEMT device performance based on analytical and numerical analyses found in the literature. For example, *I-V* characteristics of HEMTs [3], two-dimensional electron gas (2DEG) estimation [4], short channel current collapse effect [5], capacitance calculation [6], and thermal effects [7] on HEMTs have been discussed in Section 4, which have been obtained using analytical study. Section 5 includes more rigorous methods such as drift-diffusion modeling [8], transport calculation [9], Monte Carlo simulation [10], Green's function formalism [11], and polarization-based shear stress analysis [12] that need significant numerical techniques to characterize HEMT device performance. Looking back into the very recent years, some up-to-date results have been presented in Section 6, namely "Latest Research" section. Section 7 presents some prediction on the future research trends based on these latest results. Finally, possible application fields of HEMT devices have been discussed in the last section.

2. Common HEMT structures

2.1. GaAs-based HEMTs

A typical GaAs-based HEMT structure is shown in **Figure 1**. With a view to separating the majority carriers from ionized impurities, an abrupt hetero-structure is created between the

http://dx.doi.org/10.5772/67796

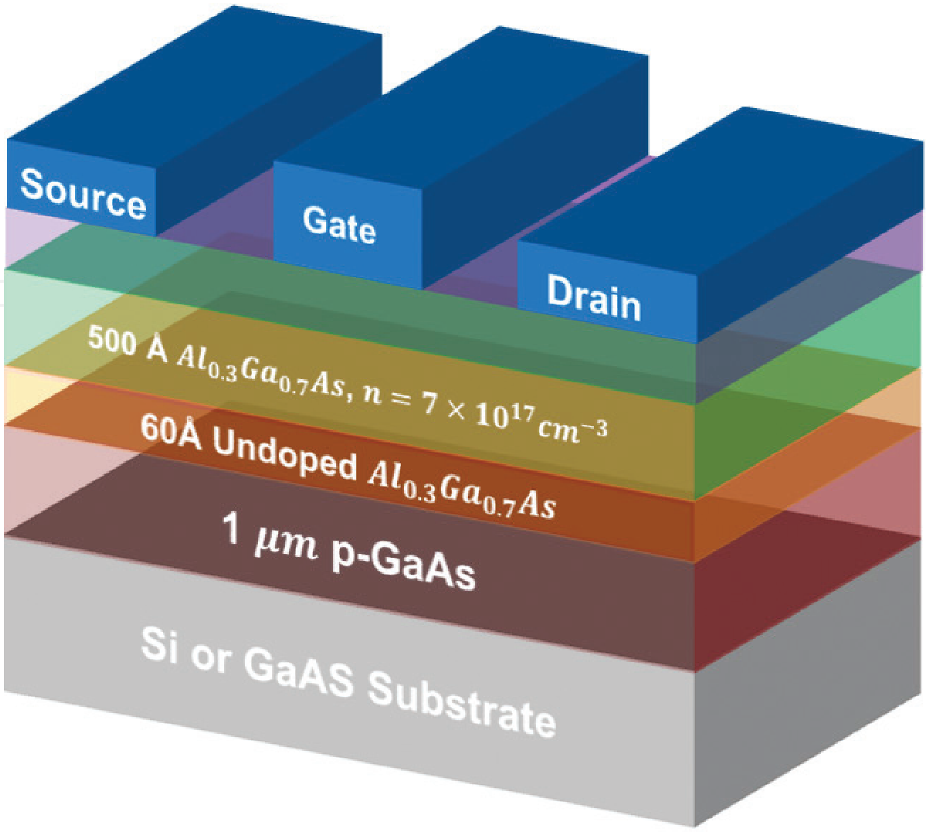

Figure 1. Structure of GaAs-based HEMTs.

wide bandgap material AlGaAs and lower bandgap material GaAs while the wide bandgap material is doped (e.g., doping density, $n = 7 \times 10^{17}$ cm^{-3}). Thus, a channel is formed at the interface of GaAs/AlGaAs heterojunction. To reduce coulombic scattering, a thin layer of undoped AlGaAs is used as spacer layer. At the bottom, the Si or GaAs layer serves as a substrate.

2.2. GaN-based HEMTs

GaN-based HEMTs have the similar layered structure to conventional GaAs-based HEMTs as shown in **Figure 2**. But no intentional doping is required in AlGaN/GaN HEMTs. Rather electrons come from surface states due to the spontaneous polarization found in wurtzite-structured GaN. This accumulation of free carrier forms high carrier concentration at the interface leads to a 2DEG channel. **Figure 2** also indicates donor-like surface traps (empty) on top and thereby the positively polarized charge at AlGaN/GaN interface. The 2DEG is an explicit function of the surface barrier, AlGaN thickness and the bound positive charge at the interface.

2.3. InP-based HEMTs

InP HEMTs result in lower electron effective mass in InGaAs channel layer compared to conventional GaAs-based HEMTs. These HEMTs contain comparatively large conduction band offset (approximately 0.5 eV) between the channel layer and adjacent barrier layer, InAlAs

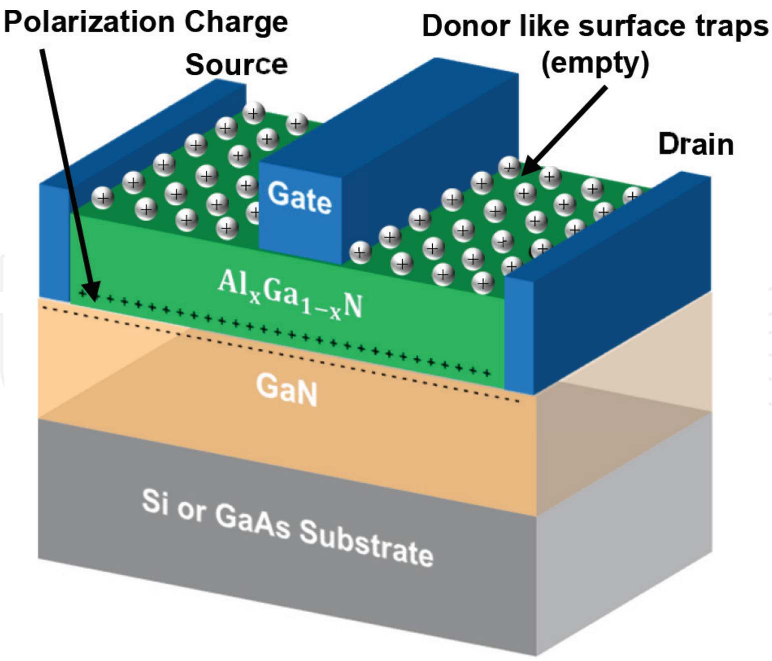

Figure 2. Structure of GaN-based HEMTs.

[13]. Hence, InP-based HEMTs show high electron mobility, high electron saturation velocity, and high electron concentration. The device usually consists of an InGaAs/InAlAs composite cap layer for enhanced ohmic contact, an undoped InAlAs as Schottky barrier and an InGaAs/InAs composite channel for superior electron transport properties as depicted in **Figure 3**.

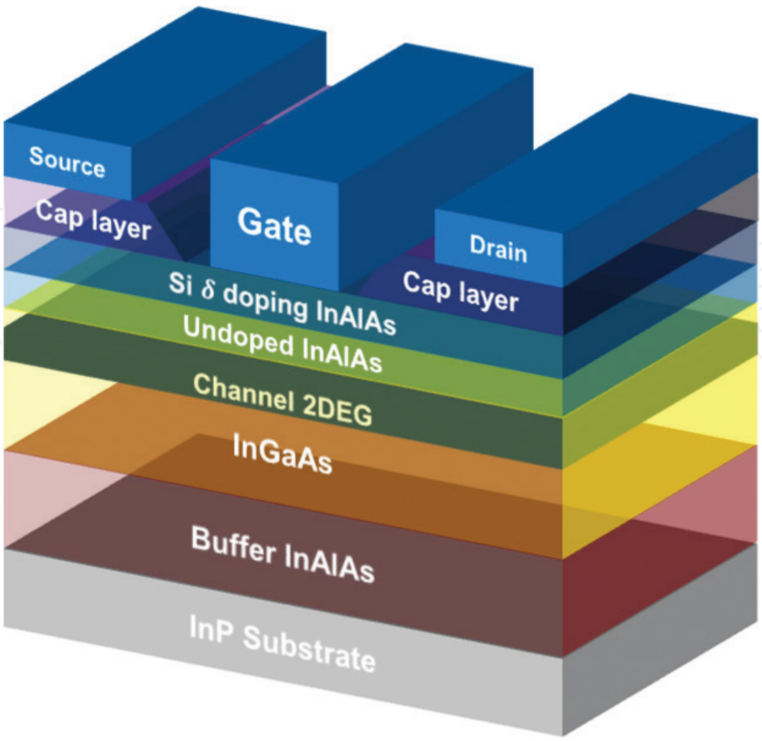

Figure 3. Structure of InP-based HEMTs.

http://dx.doi.org/10.5772/67796

3. Working principle of HEMTs

HEMTs are essentially heterojunctions formed by semiconductors having dissimilar bandgaps. When a heterojunction is formed, the conduction band and valence band throughout the material must bend to form a continuous level. The wide band element has excess electrons in the conduction band as it is doped with donor atoms (or due to polarization charge in GaN-based HEMTs). The narrow band material has conduction band states with lower energy. Therefore, electrons will diffuse from wide bandgap material to the adjacent lower bandgap material as it has states with lower energy. Thus, a change in potential will occur due to movement of electrons and an electric field will be induced between the materials. The induced electric field will drift electrons back to the conduction band of the wide bandgap element. The drift and diffusion processes continue until they balance each other, creating a junction at equilibrium like a p-n junction. Note that the undoped narrow bandgap material now has excess majority charge carriers, which yield high switching speed. An interesting fact is that the low bandgap undoped semiconductor has no donor atoms to cause scattering and thus ensures high mobility.

Another interesting aspect of HEMTs is that the band discontinuities across the conduction and valence bands can be engineered to control the type of carriers in and out of the device. This diffusion of carriers leads to the accumulation of electrons along the boundary of the two regions inside the narrow bandgap material. The accumulation of electrons can lead to a very high current in these devices. The accumulated electrons are also known as 2DEG. **Figure 4** shows the generalized band diagram formed at the heterojunction for typical HEMTs. Both

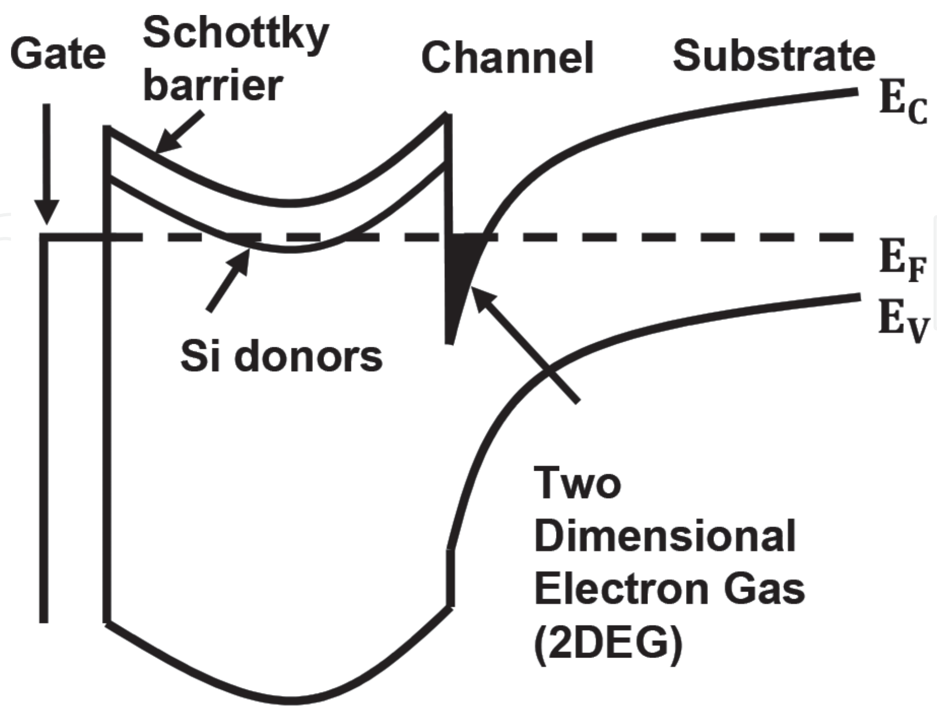

Figure 4. Generalized energy band diagram of HEMTs.

the conduction band (E_c) and valence band (E_v) bend with respect to the Fermi level (E_F) resulting in a quantum well filled with 2DEG and eventually, a conducting channel is formed.

4. Performance analysis: analytical approach

With rapidly growing popularity in high frequency and high power applications, HEMT devices have received extensive research attention in recent days. Many analytical models to study the characteristics of HEMTS as well as to improve device performance can be found in the literature. In this section, we present some of the eminent and effective analytical research works on AlGaN/GaN HEMTs.

4.1. Current-voltage characteristics using charge control model

An improved charge control model for *I-V* characteristics of AlGaN/ GaN HEMTs was presented in 2008 by Li et al. [3]. This model includes Robin boundary conditions in the solution of 1-D Schrödinger equation and customizable eigen values in the solution of 2-D Poisson's equation. Nonlinear polarization and parasitic resistance of source and drain have been incorporated in this model. The model estimates drain current assuming second-order continuity with analytical representation of transconductance. The device structure used in this model is almost similar to that of **Figure 2**. However, the only difference is that a doped AlGaN layer of 22 nm with doping concentration, $N_D = 2 \times 10^{18}$ cm^{-3} is present above the undoped AlGaN layer to enhance polarization. The *I-V* result plotted using this analytical model is shown here in **Figure 5** for different gate voltages.

4.2. Dependence of 2DEG charge density on gate bias

Khandelwal et al. proposed a physics-based analytical model for 2DEG density in AlGaN/GaN HEMTs [4]. Using this model, they show the interdependence between 2DEG and Fermi levels. The proposed model does not require any fitting parameters. It models 2DEG considering charge concentration in two different regions. One has higher first subband energy, while the other has lower first subband energy compared to the Fermi level. Moreover, a unified model is also presented combining these two regions. It presents variation of 2DEG with gate bias voltage as shown in **Figure 6**. The results show excellent agreement with numerical calculations.

4.3. Short channel *I-V*characteristics with current collapse

Current collapse is an undesirable but inevitable phenomenon in GaN-based HEMTs. It is a short channel nonideal effect where current depends on the previous memory of gate voltage. For *I-V* characteristics of AlGaN/GaN HEMTS in presence of current collapse, another compact model was proposed [5]. It incorporates trapping mechanism and gate edges and is based on experimental data. Capacitance-voltage (*C-V*) characteristics of AlGaN/ GaN HEMTs can also be calculated using this model. This model analyses device transconductance vs. gate bias when current collapse occurs. A comparative plot of transconductance with and without current collapse as determined by this compact short channel model is shown in **Figure 7**.

http://dx.doi.org/10.5772/67796

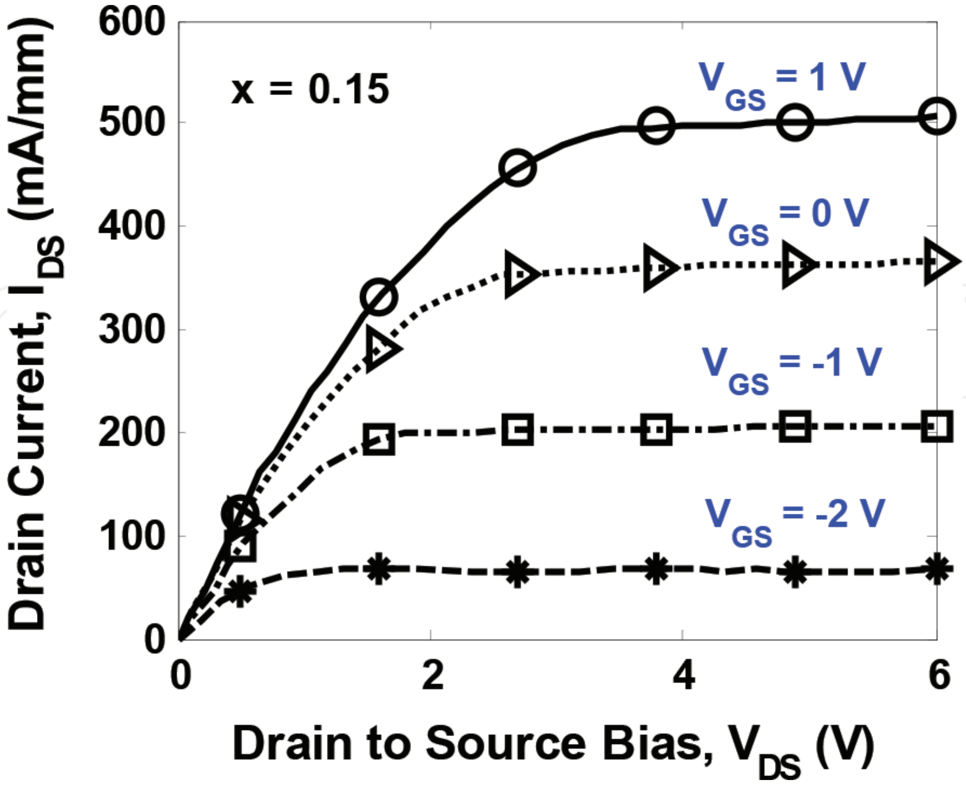

Figure 5. *I–V* characteristics for an $Al_{0.15}Ga_{0.85}N$/GaN HEMTs. The gate-to-source bias is swept from 1 to −2 V at a step of −1 V.

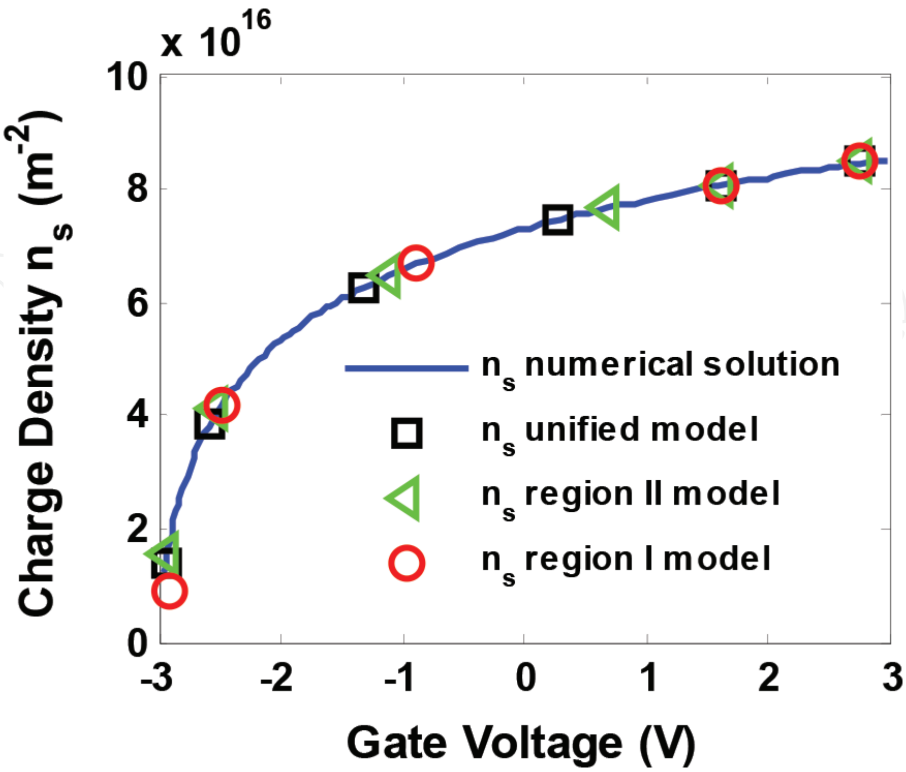

Figure 6. Comparison of 2DEG charge density, n_s with numerical calculations as a function of gate voltage.

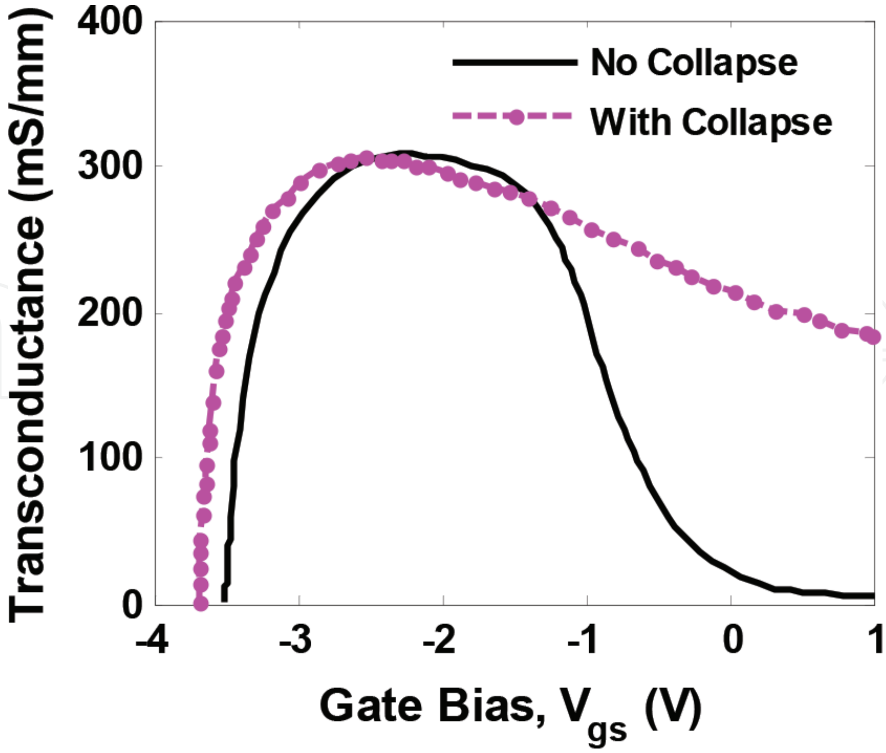

Figure 7. Comparison of transconductance with and without current collapse for AlGaN/GaN HEMTs.

4.4. Gate capacitance including parasitic components

Zhang et al. proposed a surface potential-based analytical model for calculating capacitance including parasitic components for AlGaN/GaN HEMTs [6]. The sheet charge density is modeled solving charge control equations and capacitance is calculated based on the concept of surface charge potential, which is consistent with the sheet charge density model. The parasitic components are further included in the model to provide a complete model. The developed model shows agreement with TCAD simulations and experimental data.

4.5. Thermal effects with complex structures

Although AlGaN/GaN HEMT is a promising device for high frequency and high power applications, its performance can be degraded at high temperatures. Therefore, a thermal modeling is required to predict device performance at different temperatures. Bagnall et al. developed such a thermal model that incorporates thermal effects with closed form analytical solutions for complex multilayer structured HEMTs [7]. This structure consists of N number of layers (j = 1, 2, 3, …, N) and a heat source placed within the layers as shown in **Figure 8(a)**. The analytical modeling is carried out using Fourier series solution and validated using Raman thermography spectra. Distribution of temperature along AlGaN/GaN x-axis interface including heat source as presented by the model is shown in **Figure 8(b)**.

Apart from these models, many other analytical models have been proposed for noise elimination, loss calculation, estimation of polarization, small signal analysis, etc.

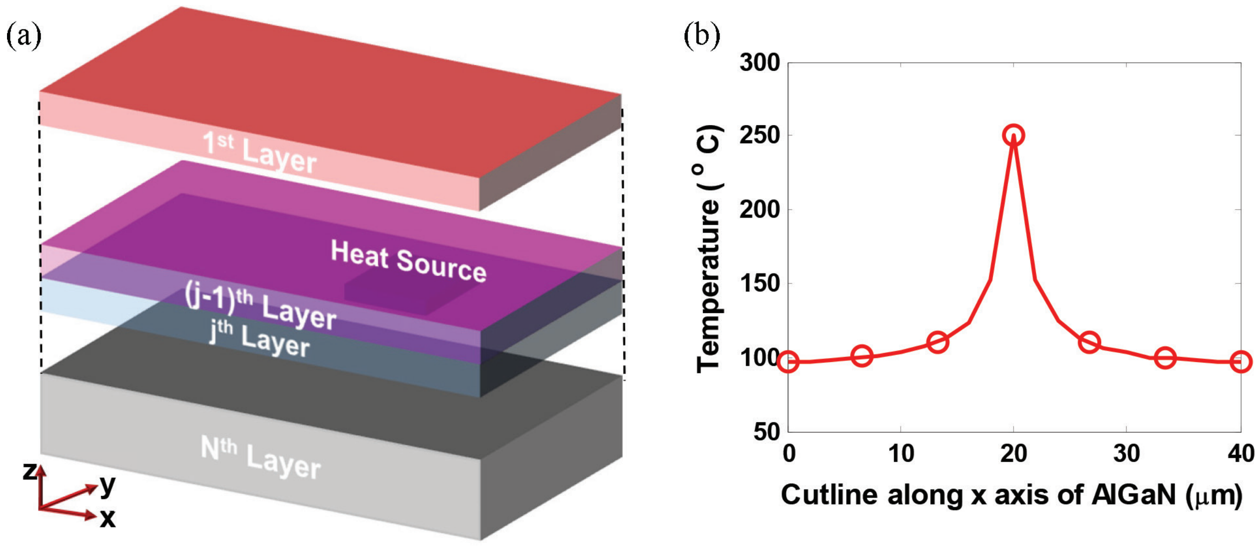

Figure 8. (a) Complex multi-layer HEMT structure with a heat source, and (b) Temperature distribution along *x* axis for AlGaN/GaN HEMTs including the heat source.

5. Performance analysis: numerical approach

Different numerical studies of HEMTs have been performed to analyze the influence of internal physical mechanisms. Some generalized numerical models reviewed from the literature are presented in this section.

5.1. Fully coupled drift-diffusion model

Yoshida et al. presented a two-dimensional numerical analysis of HEMTs to simulate device performance [8]. Anderson's model is used to generate the equations of band-edge lines and Boltzmann statistics is considered. Spatially continuous band-edge variation is not justified in this model as current across the hetero interface is neglected. The hole current and the generation-recombination current are also neglected. Finite difference approximation is used to discretize Poisson's equation and electron current continuity equation. After that, resultant equations are solved self consistently using Newton's method. This fully coupled model is traditionally known as drift-diffusion model [14].

5.2. Energy-transport model: transport calculation

Buot presented a two-dimensional numerical simulator based on the analysis of the first three moments of the Boltzmann equation, known as the energy-transport model [9]. It has been used to study various effects on the performance of AlGaAs/GaAs HEMTs [9]. The coupled transport equations (for details of energy transport equations, see Ref. [15]) were solved numerically using finite-difference technique on a uniform mesh, using iterative scheme. Using HISSDAY, a computer simulator program, the transport equations for the energy transport model are numerically solved using implicit scheme for the continuity equations; Scharfetter-Gummel method [16] for the current transport equation; and explicit forward differencing "marching" method for calculating the average energy. This model has an improvement over Widiger's energy transport model [17] where conduction is ignored in the AlGaAs layer [9].

5.3. Monte Carlo simulation

Ueno et al. presented Monte Carlo simulation of HEMTs to analyze 2DEG electron transport [10]. The analysis is based on electron–phonon interaction model proposed by Price [18]. In this framework, the 2DEG electrons are assumed to be scattered by bulk phonons. Thus, wave functions calculated by self-consistent analysis are used to evaluate the scattering rate. The channel region is not considered uniform and electrons near drain region are considered as three dimensional and near-source region are considered as two dimensional. In addition, electrons with high energy beyond the barrier height behave as three-dimensional electrons and are not confined in the quantum well. In these simulations, the initial condition is first evaluated. Then the sheet electron density at each position between the source and the drain are estimated using the current continuity relation along the channel. Next, Monte Carlo simulation is carried out by dividing the channel into different meshes and evaluating the scattering rates of the electronic states in each mesh. Then taking the potential distribution of the given device from two-dimensional Poisson equation, the steps are repeated until a steady state is obtained.

5.4. Noise current using Green's function formalism

Lee and Webb described a numerical approach to simulate the intrinsic noise sources within HEMTs [11]. A 2-D numerical device solver is used in this model. Spectral densities for the gate and drain noise current sources and their correlation are evaluated by capacitive coupling. After solving Poisson's and the continuity equations using 2-D numerical device solver, Green's functions are obtained. Here, Green's functions are used to determine local fluctuation (in terms of current or voltage at any point in the channel) at the gate and drain terminals. This approximate impedance field concept [19] helps determining the gate and drain noise sources and their correlation. For numerical simulation, the entire device is divided into some orthogonal areas and it is considered that 2-D simulation results will be consistent with the 3D simulation result. Spontaneous polarization and strain-induced piezoelectric polarization are also considered. It is assumed that the microscopic fluctuations in each segment are spatially uncorrelated which are originated from velocity fluctuation (diffusion) noise only.

5.5. High temperature shear stress analysis

Hirose et al. proposed a numerical model for AlGaN/GaN HEMT structures where shear stress due to the inverse piezoelectric effect is used to predict high-temperature DC stress test results [12]. In this model, lattice plane slip in the crystal is assumed to be the initial stage of crack formation. Shear stress causes the slip, and slip deforms the crystal when the shear stress exceeds the yield stress. In GaN-based HEMTs, the basal slip plane is (0001) and the slip direction is <1120>. The AlGaN layer is a wurtzite crystal grown in the <0001> direction [20]. Shear stress is assumed to be a result of the inverse piezoelectric effect. The mechanical stress and electric displacement occur due to the piezoelectric effect. Under the assumption of lattice mismatch in AlGaN layer, shear stress relates to the slip in the <1120> direction. However, to calculate shear stress, electric field is obtained from two-dimensional device simulation based on Poisson's equation and drift-diffusion current continuity equations. This model includes piezoelectric charges and the difference in spontaneous polarization charges in the AlGaN/GaN interface.

Among the numerical models, any one may have advantage over other models, but also have some limitations. For example, energy transport model can include hot electron effect [14]. Drift-diffusion model cannot predict performances of submicron level gate devices [9]. Monte Carlo approach is one of the advanced approaches [21]. All of these numerical models provide unique insights into the device physics and create opportunity of performance improvement with TCAD before device fabrication.

6. Latest research

With the upsurge of popularity, research works on HEMT devices are still going on. In this section, some very recent research works published in renowned scientific literature have been briefly highlighted.

6.1. GaN HEMT-based RF tuned cavity oscillator

Hörberg et al. presented a GaN-based oscillator for X band tuned by radio frequency micro-electromechanical systems (RF-MEMS) [22]. The phase noise is reported to be reduced between the range of −140 and −129 dBc/Hz at 100 kHz offset, which is significantly low. This oscillator is suitable for reduced noise-based high frequency modulators.

6.2. A compact GaN HEMT power amplifier MMIC

A compact GaN HEMT-based X-band power amplifier MMIC has been reported with detailed performance analysis recently [23]. A good range of output power (47.5–48.7 dBm) can be obtained from this amplifier. Such amplifier can be used to build electronic systems that require airborne phased radar array or satellite transmitters. Improved output power of the amplifier also improves the stability, reliability, and performance of these electronic systems. **Figure 9** shows the output power performance in both pulse mode and continuous wave (CW) modes with frequency variation in this power amplifier.

6.3. Q-spoiling based on depletion mode HEMTs

Q-spoiling is a process where MRI coils are detuned for safety and protection. Traditionally, such decoupling or Q-spoiling is done using PIN diodes, which require high current and power drain. Lu et al. proposed an alternative technique of Q-spoiling, which replaces PIN diodes with depletion mode GaN HEMTs [24]. It is shown that the proposed technology detunes MRI coils effectively with low current and power drain compared to the traditional Q-spoiling technologies. It also provides suitable safety measures required for detuning the MRI coils.

6.4. GaN HEMT oscillators with low phase noise

Excellent figure of merit (FOM) has been achieved for low phase noise in designing GaN HEMT-based oscillators [25]. The design demonstrated that low phase noise can coincide

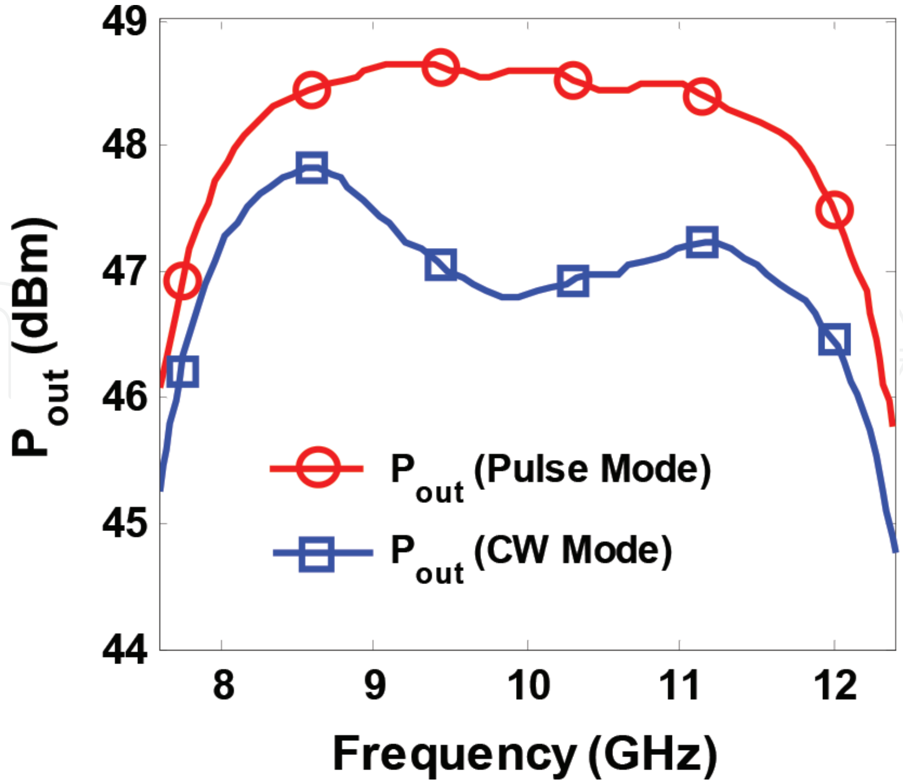

Figure 9. Output power performance of GaN HEMT power amplifier MMIC with frequency variation in pulse and CW modes.

with low bias power. The result is verified designing Colpitt and negative resistance oscillators and both of these present so far the best reported FOMs.

6.5. Kink effect in GaN HEMT technology

Crupi et al. investigated Kink effect (KE) in advanced GaN HEMT technology [26]. For better understanding, KE is studied comprehensively with change of temperature and bias conditions. It is shown that the dependence of KE on operating conditions is mainly due to device transconductance. Characterization of anomalous KE would be a useful tool for microwave engineers who need this knowledge of KE for designing and modeling devices with GaN HEMTs.

6.6. 600 V GaN HEMT switches for power converters

A total of 600 V GaN HEMT switches have been demonstrated experimentally to show performance comparison with silicon-based transistor switches such as IGBTs and MOSFETs [27]. HEMT switches, despite being beginners, show excellent performance compared to the matured counterparts, Si-based MOSFETs. It is shown that GaN switches offer higher boost converter efficiency than the MOSFET switches. Next, GaN switches are compared experimentally with IGBTs. Both Si body and SiC body-based IGBTs have been considered. It is found that at higher switching frequency, IGBT switches loss efficiency very rapidly, while HEMT switches loss efficiency monotonically as shown in **Figure 10**. Therefore, HEMTs offer superior performance to Si-based MOSFETs and IGBTs for high frequency power converter switching applications.

http://dx.doi.org/10.5772/67796

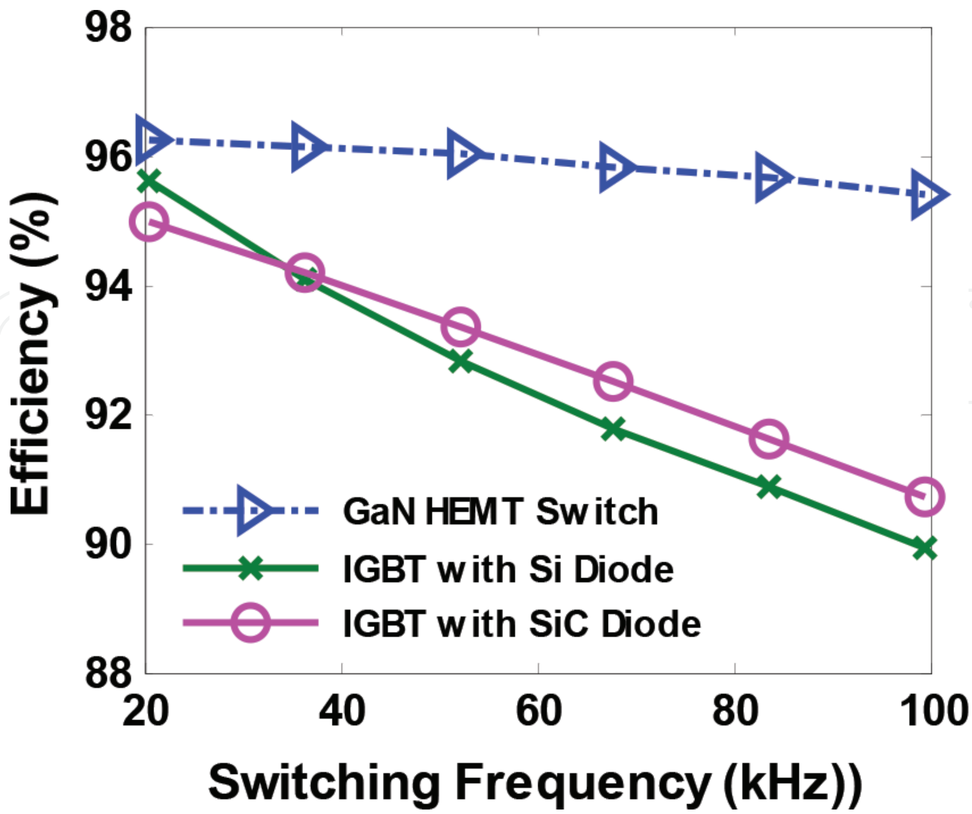

Figure 10. Comparison of efficiency for GaN HEMT switches with Si body IGBT and SiC body IGBT switches.

7. Future trends

The future HEMT devices based on two-dimensional carrier confinement seem very bright in electronics, communications, physics, and other disciplines. GaAs, InP, and GaN-based HEMTs will continue their journey toward higher integration, higher frequency, higher power, higher efficiency, lower noise, and lower cost. GaN, in particular, offers high-power, high-frequency territory of vacuum tubes and leads to lighter, more efficient, and more reliable communication systems.

HEMTs will continue to mold themselves into other kinds of FETs that will exploit the unique properties of 2DEG in various materials systems. In power electronics, GaN-based HEMTs can create a great impact on consumer, industrial, transportation, communication, and military systems. On the other hand, MOS-HEMT or MISFET structures are likely to be operated in enhancement mode with very low leakage current.

Si CMOS technology is rapidly advancing toward 10 nm gate regime. To achieve this, power dissipation management in future generation ultra-dense chips will be a significant challenge. Operating voltage reduction may be a solution to meet this challenge. However, currently, it is difficult to accomplish this with Si CMOS while maintaining quality performance. Quantum well-based devices such as InGaAs or InAs HEMTs offer very high potential. Therefore, HEMTs may extend the Moore's law for several more years which will be gigantic for the society [28].

From the past, it can be anticipated that, researching on new device models and structures of HEMTs will definitely result in new insights into the often bizarre physics of quantized electrons. ZnO, SiGe, and GaN have shown fractional quantum Hall effect (FQHE), the greatest exponent for impeccable purity and atomic order, which ensure the bright future of HEMT devices [29].

The concept of different kinds of physical and biosensors are still very new to these kind of devices. The ultra-high mobility that is possible in InAlSb/InAsSb-based system enables high-sensitivity micro-Hall sensors for many applications including scanning Hall probe microscopy and biorecognition [30]. Three-axis Hall magnetic sensors have been reported in micromachined AlGaAs/GaAs-based HEMTs [31]. These devices may be used in future electronic compasses and navigation. THz detection, mixing and frequency multiplication can also be used by 2DEG-based devices [32]. GaN and related materials have strong piezoelectric polarization, and they are also chemically stable semiconductors. Combining functionalized GaN-based 2DEG structures with free-standing resonators, there is a possibility of designing sophisticated sensors [33]. These can offer methods of measurements of several properties such as viscosity, pH, and temperature.

Without references, expansion of this technology in the machine to machine (M2M) field is expected to be used in cloud networking-based various sensing functions. Diverse applications such as environmental research, biotechnology, and structural analysis can be greatly benefited with the help of newly emerged sensing technology which has high speed, high mobility, and high sensitivity characteristics. HEMT technology is expected to make a great change in the intelligent social infrastructure from the device level. A smart city system, transport system, food industry, logistics, agriculture, health welfare, environmental science, and education systems are examples where this technology can make exceptions [34].

The rise of III-N-based solid-state lighting will lead to a continuous development of materials, substrates, and technologies pushed by a strong consumer market. In an analogy, III-N optoelectronics will challenge the light bulbs, while III-N electronics will challenge the electronic equivalent, the tubes [35].

8. Applications

Explosion of the internet multimedia communications has speedily spread over the world, which urgently demands the proliferation of transmission network capacity. HEMTs-based devices are the most attractive choices for breaking through the speed limit and high gain and noise free mechanism. Different companies worldwide develop and manufacture HEMT-based devices, and many possible applications have been suggested for these devices. Without considering all of those possibilities, some key applications are summarized in this section.

8.1. Broadband communication

Cellular communication has got the most important nonmilitary applications of HEMT devices by replacing Si transistors. For such broadband/multiband communication applications, we get a lot of advantages. The increase in relative bandwidth for a given power level is one of

http://dx.doi.org/10.5772/67796

those. Some new circuit and system concepts provide bandwidth with increased efficiency. Linearity has been improved for the same output power. Reduction of memory effects is also found by using GaN HEMT devices [36].

8.2. Radar components and space applications

High gain and low noise amplifiers are the main characteristics for making radar components. GaN HEMTs are one of the first choices for such components. Active electronic sensor arrays are built from GaN-based HEMTs, which are used for airborne radars, ground-based air defense radars, and naval radars [37]. Ka-band missile applications at 35 GHz are also being discussed in literature [38]. Discrete HEMTs are almost always used as the preamplifier in a typical DBS receiver, followed by one or more GaAs MESFET monolithic microwave integrated circuits (MMICs) due to their excellent low-noise characteristics. The use of the low-noise HEMT preamplifier has resulted in substantial improvements in system performance at little additional cost. A low-noise down-converter consisting of a 0.25 pm HEMT and three GaAs MMIC chips has shown a system noise figure less than 1.3 dB with a gain of about 62 dB from 11.7 GHz to 12.2 GHz, which is phenomenal for a commercial, system [39]. Microwave equipment used for space applications are very expensive as they need extra protection from harsh environment in space to survive. Moreover, spacecraft shall be launched, and this implies that the equipment should also sustain without damage at high levels of vibrations and shocks. HEMTs can be fabricated to survive these conditions and have been extensively used in various fields. Generally, a microwave component for space applications is ten to hundred times more expensive than for commercial applications. Workers at the National Radio Astronomy Observatory (NRAO) have used the excellent cryogenic performance of HEMTs to receive signals during the Neptune flyby of the voyager spacecraft.

8.3. Sensor applications

In the recent decade, chemical sensors have gained importance for applications that include homeland security, medical and environmental monitoring, and food safety. The desirable goal is the ability to simultaneously analyze a wide variety of environmental and biological gases and liquids in the field and be able to selectively detect a target analyte with high specificity and sensitivity. The conducting 2DEG channel of HEMTs is very close to the surface and very sensitive to adsorption of analytes. Hence, HEMT sensors can be a good alternative for detecting gases, ions, and chemicals [40].

8.4. DNA detection

Au-gated AlGaN/GaN HEMTs functionalized in the gate region with label free 3'-thiol modified oligonucleotides serves as a binding layer to the AlGaN surface, which can detect the hybridization of matched target DNAs. XPS shows immobilization of thiol modified DNA covalently bonded with gold on the gated region. Drain-source current shows a clear decrease of 115 μA as this matched target DNA is introduced to the probe DNA on the surface, showing the promise of the DNA sequence detection for biological sensing [41].

8.5. Protein detection

Using amino-propyl silane in the gate region, ungated AlGaN/GaN HEMT structures can be activated, which can serve as a binding layer to the AlGaN surface for attachment of biotin. Biotin has a very high affinity to streptavidin proteins. When the chemicals are attached to AlGaN/GaN HEMTs, the charges on the attached chemicals affect the current of the device. The device shows a clear decrease of 4 μA as soon as this protein is collected at the surface, showing indication of protein sensing [41].

8.6. pH detection

The use of Sc_2O_3 gate dielectric produces superior results to either native oxide or UV ozone-induced oxide in the gate region. The ungated HEMTs with Sc_2O_3 in the gate region exhibit a linear change in current between pH 3–10 of 37μA/pH. The HEMT pH sensors show stable operation with a resolution of <0.1 pH over the entire pH range. The results indicate that HEMTs may have application in monitoring pH solution changes between 7 and 8, the range of interest for testing human blood [40].

9. Conclusion

In this chapter, device characteristics and performance analysis of HEMTs have been discussed based on the available literature. With a brief introduction of different structures and brief working principle, this chapter summarizes some prominent analytical and numerical research works on HEMTs. *I-V* characteristics, charge estimation, capacitance calculation, short channel effects, and thermal response of HEMTs have been discussed. Moreover, drift diffusion modeling, transport calculation, Monte Carlo simulation, Green's function formalism, and shear stress analysis have been discussed which rely on numerical approaches. HEMT-based oscillators, amplifiers, Q-spoilers, switches, and diodes are getting popularity in recent days. These have been overviewed based on latest reported researches. Based on these latest research studies, future research trends on HEMTs have been reviewed. Last but not the least, many important applications of HEMTs such as broadband and radar communications, space, and sensor constituents, DNA, protein, and pH detections have been listed to emphasize the immense prospects of HEMT devices. This chapter provides researchers of relevant fields a direction for future improvement of HEMT devices with prospective applications.

Author details

Muhammad Navid Anjum Aadit, Sharadindu Gopal Kirtania, Farhana Afrin, Md. Kawsar Alam* and Quazi Deen Mohd Khosru

*Address all correspondence to: kawsaralam@eee.buet.ac.bd

Department of Electrical and Electronic Engineering, Bangladesh University of Engineering and Technology, Dhaka, Bangladesh

http://dx.doi.org/10.5772/67796

References

[1] Mimura T. The early history of the high electron mobility transistor (HEMT). IEEE Transactions on Microwave Theory and Techniques. 2002 Mar;50(3):780–2.

[2] Gangwani P, Pandey S, Haldar S, Gupta M, Gupta RS. Polarization dependent analysis of AlGaN/GaN HEMT for high power applications. Solid-State Electronics. 2007 Jan 31;51(1):130–5.

[3] Li M, Wang Y. 2-D analytical model for current–voltage characteristics and transconductance of AlGaN/GaN MODFETs. IEEE Transactions on Electron Devices. 2008 Jan;55(1):261–7.

[4] Khandelwal S, Goyal N, Fjeldly TA. A physics-based analytical model for 2DEG charge density in AlGaN/GaN HEMT devices. IEEE Transactions on Electron Devices. 2011 Oct;58(10):3622–5.

[5] Koudymov A, Shur MS, Simin G, Chu K, Chao PC, Lee C, Jimenez J, Balistreri A. Analytical HFET *I-V* model in presence of current collapse. IEEE Transactions on Electron Devices. 2008 Mar;55(3):712–20.

[6] Zhang A, Zhang L, Tang Z, Cheng X, Wang Y, Chen KJ, Chan M. Analytical modeling of capacitances for GaN HEMTs, including parasitic components. IEEE Transactions on Electron Devices. 2014 Mar;61(3):755–61.

[7] Bagnall KR, Saadat OI, Palacios T, Wang EN. Analytical thermal model for HEMTs with complex epitaxial structures. In: 2014 IEEE Intersociety Conference on Thermal and Thermomechanical Phenomena in Electronic Systems (ITherm), 2014 May 27–30 (pp. 947–958), Orlando, FL, USA. IEEE.

[8] Yoshida J, Kurata M. Analysis of high electron mobility transistors based on a two-dimensional numerical model. IEEE Electron Device Letters. 1984 Dec;5(12):508–10.

[9] Buot FA. Two-dimensional numerical modelling of HEMT using an energy transport model. COMPEL-The International Journal for Computation and Mathematics in Electrical and Electronic Engineering. 1987 Jan 1;6(1):45–52.

[10] Ueno H, Yamakawa S, Hamaguchi C, Miyatsuji K. Monte Carlo simulation of HEMT. In: Proceedings, IEEE International Workshop on Physics and Computer Modeling of Devices Based on Low-Dimensional Structures. 1995 Nov 7 (pp. 85–89), Aizu-Wakamatsu, Japan. IEEE.

[11] Lee S, Webb KJ. Numerical noise model for the AlGaN/GaN HEMT. In: 2004 IEEE MTT-S International Microwave Symposium Digest, 2004 Jun 6 (Vol. 2, pp. 1057–1060), Fort Worth, TX, USA. IEEE.

[12] Hirose M, Matsushita K, Takagi K, Tsuda K. Numerical device model for reliable AlGaN/GaN HEMT structure design based on shear stress. In: 2013 IEEE Compound Semiconductor Integrated Circuit Symposium (CSICS), 2013 Oct 13 (pp. 1–4), Monterey, CA, USA. IEEE.

[13] Shinohara K, Matsui T. 3–7 Nano-gate transistor-world's fastest InP-HEMT. Journal of the National Institute of Information and Communications Technology. 2004;51:95–102.

[14] Loret D. Two-dimensional numerical model for the high electron mobility transistor. Solid-State Electronics. 1987 Nov 1;30(11):1197–203.

[15] Portengen T, Boots HM, Schuurmans MF. A priori incorporation of ballistic and heating effects in a four-moment approach to the Boltzmann equation. Journal of Applied Physics. 1990 Sep 15;68(6):2817–23.

[16] Glover GH. Study of electron energy relaxation times in GaAs and InP. Journal of Applied Physics. 1973 Mar;44(3):1295–301.

[17] Widiger D, Hess K, Coleman JJ. Two-dimensional numerical analysis of the high electron mobility transistor. IEEE Electron Device Letters. 1984 Jul;5(7):266–9.

[18] Price PJ. Two-dimensional electron transport in semiconductor layers. I. Phonon scattering. Annals of Physics. 1981 May 1;133(2):217–39.

[19] Shockley W, Copeland JA, James RP. The impedance field method of noise calculation in active semiconductor devices. Quantum Theory of Atoms, Molecules, and the Solid State, A Tribute to John C. Slater. Edited by Per-Olov Löwdin. New York: Academic Press, USA, 1966, p.537.

[20] Paufler P. RWK Honeycombe: The plastic deformation of metals. Edward Arnold (Publ.) ltd., Maidenhead, 1984, 483 p., paperback. ISBN 0713134682.

[21] Snowden CM. Compound Semiconductor Device Modelling. Miles RE, editor. Springer-Verlag; London, UK 1993 Mar.

[22] Hörberg M, Emanuelsson T, Ligander P, Lai S, Zirath H, Kuylenstierna D. RF-MEMS tuned GaN HEMT based cavity oscillator for X-band. IEEE Microwave and Wireless Components Letters. 2017 Jan; 27(1); 46–48.

[23] Tao HQ, Hong W, Zhang B, Yu XM. A compact 60W X-band GaN HEMT power amplifier MMIC. IEEE Microwave and Wireless Components Letters. 2017 Jan; 27(1); 73–75.

[24] Lu JY, Grafendorfer T, Zhang T, Vasanawala S, Robb F, Pauly JM, Scott GC. Depletion-mode GaN HEMT Q-spoil switches for MRI coils. IEEE Transactions on Medical Imaging. 2016 Dec;35(12):2558–67.

[25] Lai S, Kuylenstierna D, O¨zen M, Horberg M, Rorsman N, Angelov I, Zirath H. Low phase noise GaN HEMT oscillators with excellent figures of merit. IEEE Microwave and Wireless Components Letters. 2014 Jun;24(6):412–4.

[26] Crupi G, Raffo A, Marinkovic Z, Avolio G, Caddemi A, Markovic V, Vannini G, Schreurs DM. An extensive experimental analysis of the kink effects in S_{22} and h_{21} for a GaN HEMT. IEEE Transactions on Microwave Theory and Techniques. 2014 Mar;62(3):513–20.

[27] Mitova R, Ghosh R, Mhaskar U, Klikic D, Wang MX, Dentella A. Investigations of 600-V GaN HEMT and GaN diode for power converter applications. IEEE Transactions on Power Electronics. 2014 May;29(5):2441–52.

[28] Del Alamo, Jesus A. The High-Electron Mobility Transistor at 30: Impressive Accomplishments and Exciting Prospects. In: 2011 International Conference on Compound Semiconductor Manufacturing Technology, 2011 May (pp. 16-19), Indian Wells, California, USA. IEEE.

[29] Chen YZ, Trier F, Wijnands T, Green RJ, Gauquelin N, Egoavil R, Christensen DV, Koster G, Huijben M, Bovet N, Macke S. Extreme mobility enhancement of two-dimensional electron gases at oxide interfaces by charge-transfer-induced modulation doping. Nature Materials. 2015 Aug 1;14(8):801–6.

[30] Bando M, Ohashi T, Dede M, Akram R, Oral A, Park SY, Shibasaki I, Handa H, Sandhu A. High sensitivity and multifunctional micro-Hall sensors fabricated using InAlSb/InAsSb/InAlSb heterostructures. Journal of Applied Physics. 2009 Apr 1;105(7):07E909.

[31] Vorob'ev A, Chesnitskiy A, Toropov A, Prinz V. Three-axis Hall transducer based on semiconductor microtubes. Applied Physics Letters. 2013 Oct 21;103(17):173513.

[32] Dyakonov M, Shur M. Detection, mixing, and frequency multiplication of terahertz radiation by two-dimensional electronic fluid. IEEE Transactions on Electron Devices. 1996 Mar;43(3):380–7.

[33] Brueckner K, Niebelschuetz F, Tonisch K, Michael S, Dadgar A, Krost A, Cimalla V, Ambacher O, Stephan R, Hein MA. Two-dimensional electron gas based actuation of piezoelectric AlGaN/GaN microelectromechanical resonators. Applied Physics Letters. 2008 Oct 27;93(17):173504.

[34] Joshin K, Kikkawa T, Masuda S, Watanabe K. Outlook for GaN HEMT technology. Fujitsu Scientific and Technical Journal. 2014 Jan 1;50(1):138–43.

[35] Quay R. Gallium Nitride Electronics. Springer Science & Business Media; Berlin, Germany 2008 Apr 5.

[36] Wen CP, Wang J, Hao Y. Current collapse, memory effect free GaN HEMT. In: 2010 IEEE MTT-S International Microwave Symposium Digest (MTT), 2010 May 23 (pp. 149–152), Anaheim, CA, USA. IEEE.

[37] Mancuso Y, Gremillet P, Lacomme P. T/R-modules technological and technical trends for phased array antennas. In: 2005 European Microwave Conference, 2005 Oct 4-6 (pp. 614–617), Paris, France. IEEE.

[38] Hommel H, Feldle H. Current status of airborne active phased array (AESA) radar systems and future trends. In: 34th European Microwave Conference, 2004 Oct 12-14 (pp. 121–124, Amsterdam, Netherlands. IEEE.

[39] Kiehl RSollner T. High Speed Heterostructure Devices. 1st ed. Boston: Academic Press; 1994.

[40] Chu BH, Kang BS, Wang HT, Chang CY, Tseng Y, Goh A, Sciullo A, Wu WS, Lin JN, Gila BP, Pearton SJ. AlGaN/GaN HEMT and ZnO nanorod-based sensors for chemical and bio-applications. In: SPIE OPTO: Integrated Optoelectronic Devices 2009 Feb 12 (pp. 72162A–72162A). San Jose, CA, USA. International Society for Optics and Photonics.

[41] Kang BS. Fabrication and Characterization of Compound Semiconductor Sensors for Pressure, Gas, Chemical, And Biomaterial Sensing (Doctoral dissertation, University of Florida).

IntechOpen